

THE SUPER-SOFT X-RAY PHASE OF NOVA RS OPHIUCHI 2006

J.P. OSBORNE¹, K.L. PAGE¹, A.P. BEARDMORE¹, M.F. BODE², M.R. GOAD¹, T.J. O'BRIEN³, S. STARRFIELD⁴, T. RAUCH⁵, J.-U. NESS⁶, J. KRAUTTER⁷, G. SCHWARZ⁸, D.N. BURROWS⁹, N. GEHRELS¹⁰, J.J. DRAKE¹¹, A. EVANS¹² AND S.P.S. EYRES¹³

Draft version November 25, 2010

ABSTRACT

Swift X-ray observations of the ~ 60 day super-soft phase of the recurrent nova RS Ophiuchi 2006 show the progress of nuclear burning on the white dwarf in exquisite detail. First seen 26 days after the optical outburst, this phase started with extreme variability likely due to variable absorption, although intrinsic white dwarf variations are not excluded. About 32 days later, a steady decline in count-rate set in. NLTE model atmosphere spectral fits during the super-soft phase show that the effective temperature of the white dwarf increases from ~ 65 eV to ~ 90 eV during the extreme variability phase, falling slowly after about day 60 and more rapidly after day 80. The bolometric luminosity is seen to be approximately constant and close to Eddington from day 45 up to day 60, the subsequent decline possibly signalling the end of extensive nuclear burning. Before the decline, a multiply-periodic, ~ 35 s modulation of the soft X-rays was present and may be the signature of a nuclear fusion driven instability. Our measurements are consistent with a white dwarf mass near the Chandrasekhar limit; combined with a deduced accumulation of mass transferred from its binary companion, this leads us to suggest RS Oph is a strong candidate for a future supernova explosion. The main uncertainty now is whether the WD is the CO type necessary for a SN Ia. This may be confirmed by detailed abundance analyses of spectroscopic data from the outbursts.

Subject headings: novae — binaries: symbiotic — stars: oscillations — X-rays: individual (RS Oph)

1. INTRODUCTION

Novae result from the explosive thermonuclear fusion of hydrogen to helium in the surface layers of a white dwarf (WD). The hydrogen-rich fuel for this process is provided by accretion from the outer layers of a cooler binary companion (Starrfield 2008), in the case of RS Ophiuchi (RS Oph), a red giant (RG). Most novae have a single historically recorded outburst (the Classical Novae [CNe]), but a few, including RS Oph, are recurrent on timescales of ~ 8 to less than 80 years – the so-called Recurrent Novae (RNe; see Schaefer 2010 for a review). The observably short recurrence intervals for RNe are thought to result from a higher accretion rate and a higher WD

mass than in CNe, both leading to a more rapid release of energy in the ignition zone and a shorter time to runaway (Townsley 2008).

RS Oph shows recurrent nova outbursts at roughly 20 year intervals. The latest outburst was detected on 2006 Feb 12.8 at a magnitude of 4.5 (Narumi et al. 2006; see Hounsell et al. 2010 for a complete early light curve). Multi-frequency observations during the previous outburst in 1985 led to determinations of the distance, $d = 1.6 \pm 0.3$ kpc (Bode 1987), and the interstellar column density, $N_{\text{H,ISM}} = (2.4 \pm 0.6) \times 10^{21} \text{ cm}^{-2}$ (Hjellming et al. 1986). X-ray observations were conducted by *EXOSAT* at six epochs, from days 55 to 251 after the outburst, over the 0.04–2.0 keV and 1.5–15 keV bands (Mason et al. 1987; O'Brien et al. 1992). X-ray emission during the first five epochs was consistent with shocks propagating through the pre-existing wind of the RG companion star. Modelling this process, O'Brien et al. (1992) derived an outburst energy of 1.1×10^{43} erg and an ejected mass of $1.1 \times 10^{-6} M_{\odot}$, but it proved difficult to model the low and high energy X-ray evolution simultaneously and the authors suggested that on-going nuclear fusion on the WD surface might be responsible. As will be shown in this paper, our results confirm this view.

Novae have been predicted to undergo a super-soft source (SSS) phase as the mass loss from the central source declines and the effective photospheric surface shrinks at constant bolometric luminosity (MacDonald et al. 1985). This phase, which produces emission from the surface of the WD with temperatures around 3×10^5 K, has been observed in several novae; see, e.g., Page et al. (2010); Drake et al. (2003); Ness et al. (2003); Orio et al. (2002). Previously, the outburst of V1974 Cyg in 1992 had the best temporal coverage, with 18 epochs

julo@star.le.ac.uk

¹ Department of Physics and Astronomy, University of Leicester, Leicester, LE1 7RH, UK

² Astrophysics Research Institute, Liverpool John Moores University, Birkenhead, CH41 1LD, UK

³ Jodrell Bank Observatory, School of Physics & Astronomy, University of Manchester, Macclesfield, SK11 9DL, UK

⁴ School of Earth and Space Exploration, Arizona State University, P.O. Box 871404, Tempe, AZ 85287-1404, USA

⁵ Institute for Astronomy and Astrophysics, Kepler Center for Astro and Particle Physics, Eberhard Karls University, Sand 1, D-72076 Tübingen, Germany

⁶ XMM-Newton Science Operations Centre, ESAC, Apartado 78, 28691 Villanueva de la Cañada, Madrid, Spain

⁷ Landessternwarte, Königstuhl, 69117 Heidelberg, Germany

⁸ American Astronomical Society, 2000 Florida Ave, NW, Suite 400, Washington, DC 20009-1231, USA

⁹ Department of Astronomy and Astrophysics, Pennsylvania State University, University Park, Pennsylvania, 16802, USA

¹⁰ NASA Goddard Space Flight Center, Greenbelt, Maryland 20771, USA

¹¹ Smithsonian Astrophysical Observatory, 60 Garden St., MS 3, Cambridge, MA 02138, USA

¹² Astrophysics Group, School of Physical and Geographical Sciences, Keele University, Staffordshire, ST5 5BG, UK

¹³ Jeremiah Horrocks Institute, University of Central Lancashire, Preston, PR1 2HE, UK

of *ROSAT* observations ranging from 63 to 653 days after outburst (Krautter et al. 1996, Balman et al. 1998). This outburst was the brightest SSS observed at the time (in terms of observed flux), but our *Swift* data show that RS Oph peaked 2-3 times brighter still.

X-ray data from the 2006 outburst of RS Oph were obtained by *Swift*, the Rossi X-Ray Timing Explorer (*RXTE*), *XMM-Newton* and *Chandra* and have been extensively discussed in a range of papers. Bode et al. (2006) described the early hard emission, based on *Swift*-X-ray Telescope (XRT) observations (as well as a detection by the Burst Alert Telescope – the hard X-ray instrument onboard *Swift*), confirming basic models from the 1985 outburst, while Sokoloski et al. (2006) presented the *RXTE* data for a similar early time interval. Ness et al. (2007, 2009) and Nelson et al. (2008) discuss the grating spectra obtained by *XMM-Newton* and *Chandra*, both before and during the SSS phase, while Drake et al. (2009) concentrated on the early (pre-SSS) *Chandra* high-energy transmission grating alone, finding the ejecta may contain super-solar abundances. Luna et al. (2009) find evidence for extended soft X-ray emission using *Chandra* CCD data. Vaytet, O’Brien & Bode (2007) present 1-dimensional hydrodynamical models of the shocks within the interacting winds of the RS Oph system and compare them to the results of Bode et al. (2006). Their models reproduce the rise and subsequent deceleration of the shock velocities, but require a very high speed wind to achieve the high shock velocity observed. Three-dimensional modelling performed by Walder, Folini & Shore (2008) leads them to conclude that the WD mass in the RS Oph system is increasing with time. Similar conclusions were reached by Orlando et al. (2009), who estimated a total ejecta mass of $10^{-6}M_{\odot}$ based on 3-D hydrodynamical modelling constrained by *Swift* and *Chandra* X-ray observations.

Besides the X-ray observations, data on RS Oph were also collected in the radio (O’Brien et al. 2006; Kantharia et al. 2007; Eyres et al. 2009), IR (Monnier et al. 2006; Das, Banerjee & Ashok 2006; Evans et al. 2007a,b; Chesneau et al. 2007; Lane et al. 2007; Banerjee, Das & Ashok 2009; Rushton et al. 2010; Brandi et al. 2009) and optical bands (Hachisu et al. 2006; Worters et al. 2007; Bode et al. 2007; Munari et al. 2007; Brandi et al. 2009).

Hachisu, Kato & Luna (2007) discussed the temporal evolution of the RS Oph SSS X-ray light curve, but did not include any detailed consideration of the spectral characteristics or their evolution; nor did they include the effects of interstellar and (changing) circumstellar absorption on their conclusions. Here we perform spectral fits to derive physical parameters such as effective temperatures and luminosities, compare them to observational results from other wavebands and also to theoretical expectations. In addition, we explore temporal variability of the SSS on timescales down to seconds and discuss the origin and implications of our results. Finally, Hachisu et al. (2007) concluded that this system is a SN Ia progenitor. Here we reconsider this important conclusion and suggest additional analysis that is crucial to confirming or rejecting this hypothesis.

The *Swift* satellite (Gehrels et al. 2004) is a rapid-response observatory, designed for the study of Gamma-Ray Bursts (GRBs). It includes a Burst Alert Telescope (BAT, 15–350 keV; Barthelmy et al. 2005), the XRT (0.3–10 keV; Burrows et al. 2005), and a UV-optical telescope (UVOT, 170–650 nm; Roming et al. 2005). *Swift* observations started within 3.2 days of the outburst (defined as 2006 Feb 12.8) and were repeated in over 350 snap-shots between days 3 and 1565; they were scheduled according to the behaviour of the source, although GRBs occasionally interrupted. The observations consisted of short continuous snap-shots of 20–2600 s, and were made at multiples of the *Swift* orbital period of 96 min. Observations were initially made at 2–8 days spacing up to 2006 March 13 (day 29). In response to an observed dramatic count rate increase (Osborne et al. 2006a), the observation frequency was increased to one per day until 2006 March 16 (day 32), and then to many a day (up to a maximum of 18) until the end of April (day 77), after which it was reduced to around one observation every three days. From 2006 May 24 (day 100), this was then further reduced to between once a week and once a fortnight until the end of the observing window on 2006 October 22 (day 252). A further four observations were taken between days 372 and 392 (2007 February and March) when RS Oph became observable again by *Swift*, followed by ~ 10 ks between days 592–596 (end of September/beginning of October 2007), before the target again became observationally constrained. ~ 12.5 ks were collected between days 818–820 (May 2008), ~ 13.3 ks between 2009 August and September and a final short observation was made in 2010 May. The total exposure time of the observations reported here is almost 450 ks. The complete *Swift* X-ray dataset to date is plotted in Fig. 1.

Before day 90 observations were made in Windowed Timing (WT) mode, which provides one-dimensional spatial information and 1.8 ms time resolution. This mode was selected because the alternative, Photon Counting (PC) mode, with its longer integration time of 2.5 s, would have resulted in unusably piled-up data – pile-up occurs when more than one photon provides charge to a pixel before readout. WT event grades 0-2 were selected for analysis (Burrows et al. 2005), as this selection gives good efficiency and discrimination against background, and the event lists were cleaned in the standard manner using the *xrtpipeline*¹⁴ within *Swift* software version 3.4 (corresponding to HEASoft 6.7). The source data were extracted using an annulus of inner and outer radii equal to five and 30 pixels (one XRT pixel = $2.36''$). They were corrected for pile-up by normalising for the excluded central pixels (which removed up to 75% of the observed counts), and similarly for the presence of bad CCD pixels. For the light-curve, this was done through the use of the *Swift* FTOOLS *xrtlccorr*, while the ancillary response files created using *xrtmkarf* performed the same function for the spectra.

By day 90 RS Oph had faded to the point where PC mode could be used; again we used a 30 pixel outer-radius source extraction region. PC observations before

2. SWIFT XRT OBSERVATIONS AND DATA REDUCTION

¹⁴ Part of the XRT Data Analysis Software (XRTDAS) developed under the responsibility of the ASI Science Data Center (ASDC), Italy.

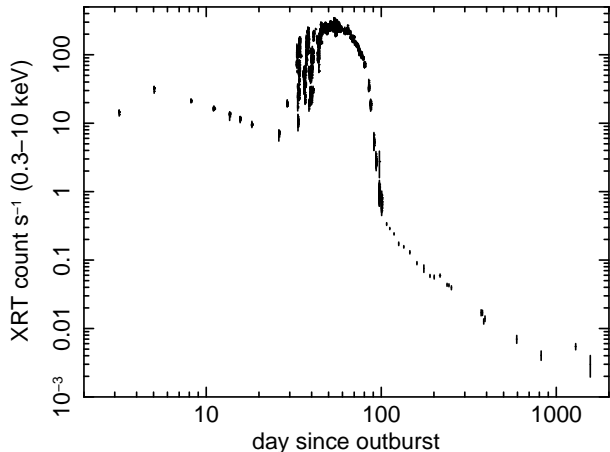


FIG. 1.— The entire 0.3–10 keV *Swift*-X-ray light-curve of RS Oph. The pile-up corrected count rate as a function of the number of days since outburst is plotted on log-log scales. The super-soft phase is prominent between days 29 and 100.

day 100 were affected by pile-up and a central exclusion region that varied from six down to zero pixels in radius was applied to select only unaffected events. PC event grades 0–12 were accumulated and corrected for the effects of excluded and bad pixels, again using *xrtlccorr* and *xrtmkarf* where appropriate. The most up-to-date version of the calibration files (version 11 of the RMFs) was used.

3. X-RAY LIGHT-CURVE AND SPECTRUM

After an initial modest increase in brightness in the second observation (Figs 1 and 2), the X-ray count rate of RS Oph slowly fell to 6 count s^{-1} on day 26. During this initial interval, the spectrum was relatively hard, characterised by the emission expected from an optically thin plasma; these early observations are described by Bode et al. (2006). The following observation on day 29 showed RS Oph at 15 count s^{-1} , beginning a phase of dramatic increase in count rate and large amplitude variations which peaked above 250 count s^{-1} (Osborne et al. 2006b); Fig. 2 shows a change from 260 to 20 count s^{-1} in ~ 12 hours during day 38. Most of the additional count rate resulted from a huge increase at energies below 0.7 keV. Around day 46 the rate stabilised, peaking at more than 300 count s^{-1} , then around day 58 a roughly linear decline began (Osborne et al. 2006c). The X-ray emission ($E < 1$ keV) seen in the period from day 26 to day 58 was very much softer than the optically thin spectrum, with $kT \sim$ a few keV, which had been seen earlier in the outburst (Fig. 3). The decline of the soft X-ray spectrum continued to about day 90, when the SSS component was no longer evident (Osborne et al. 2006d); the hardness of the spectrum, as measured by ratio of the count rates (0.6–2.0 keV/0.3–0.6 keV), started to increase again at this time, a trend which continued to day ~ 120 (Fig. 2), after which the hardness ratio stayed approximately constant.

As in CNe, this X-ray behaviour is in stark contrast to that in the optical, in which a relatively smooth decline in magnitude over ~ 140 days from the time of outburst was observed, albeit with a break in slope around day

70 (as shown by the AAVSO dataset¹⁵). While the declining X-ray flux prior to day 26 is well described by the evolution of shock systems established as the high-velocity ejecta impacted the RG wind (Bode et al. 2006; Sokoloski et al. 2006), the rapidly-appearing, bright and highly variable soft component cannot be explained by this mechanism. The very high luminosity (see below) rules out re-established accretion as the origin of this component.

The harder, shock-generated emission has a faster power-law decline after the SSS phase than before it. The maximum count rates due to this emission are below the pile-up limits for the modes used, so the light curve reflects the intrinsic behaviour of the source. Faster fading around the time of the SSS phase is suggested by the 1-D cooling model of Vaytet et al. (2007 & 2010) which show that shock breakout of the red giant wind established since the previous nova explosion can occur then, and can reproduce the faster power-law decline. However, 3-D modelling is likely to be required for a complete understanding given the complex spatial structure of the observed remnant (Bode et al. 2007, Sokoloski, Rupen & Mioduszewski 2008, Luna et al. 2009); current 3-D models (Walder, Folini & Shore 2008, Orlando, Drake & Laming 2009) unfortunately do not extend to this epoch.

High-resolution X-ray grating spectra from *Chandra* and *XMM-Newton* (Ness et al. 2007, 2009) show that the soft component was dominated by continuum emission over 0.3–0.8 keV on days 39, 53 and 66, with both emission and absorption lines superimposed, indicating a hot WD stellar atmosphere possibly with outflow. Emission features included lines attributable to the presence of H- and He-like N and H-like O.

A sample of *Swift*-XRT spectra is shown in Fig. 3 to demonstrate the large variation in spectral shape during the supersoft phase; the spectral evolution is discussed in more detail below. We note that the resolution of the XRT at 0.5 keV is only 63 eV (full width half maximum) and definitive detection of sharp spectral features requires the use of instruments with higher spectral resolution. Nevertheless, the narrow emission and absorption features due to N and O seen in the grating data by Ness et al. (2007) are also discernible in the *Swift*-XRT spectra.

We characterised the SSS spectrum by minimum χ^2 fits to the observed 0.3–10 keV spectra using XSPEC v12¹⁶. Our model consisted of a plane-parallel, non-local thermodynamic equilibrium atmosphere component (Rauch 2003; Rauch et al. 2010) and a two-temperature optically-thin solar abundance plasma to characterise the shocked wind, all absorbed by intervening gas (the column density being the sum of the interstellar and the declining absorption from the unshocked RG wind [Bode et al. 2006]). The model atmosphere grids were calculated for temperatures of $(5.5 - 10.5) \times 10^5$ K, in steps of 10^4 K. The declining column was constrained to follow a monotonic power-law decrease over time, of the form $N_{\text{H,wind}} = 7.5 \times 10^{21} t^{-0.5} \text{ cm}^{-2}$ (determined from Bode et al. 2006, their fig. 4), where t is the time since outburst in days. The two-temperature model for the optically thin component is justified in each case by the large

¹⁵ <http://www.aavso.org/>

¹⁶ <http://heasarc.gsfc.nasa.gov/docs/xanadu/xspec/index.html>

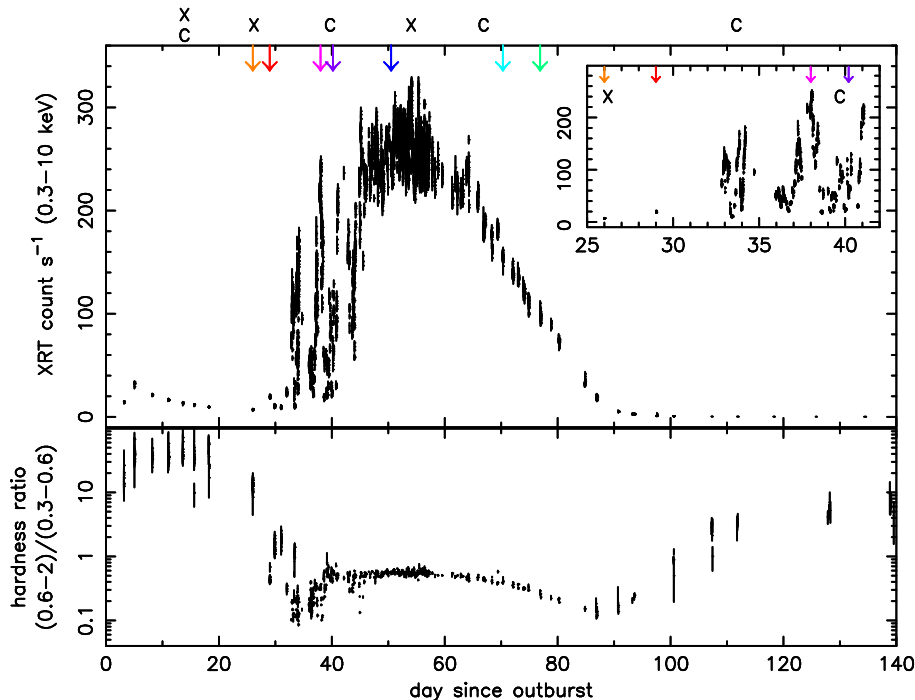


FIG. 2.— The *Swift*-XRT light-curve (top) and the (0.6–2)/(0.3–0.6) count rate hardness ratio (bottom) for RS Oph from 3 to 135 days after the outburst discovery. The times of high spectral resolution grating observations by *XMM-Newton* (X) and *Chandra* (C) are marked (e.g., Ness et al. 2007), as are the times of the XRT spectra (coloured arrows) shown in Fig. 3.

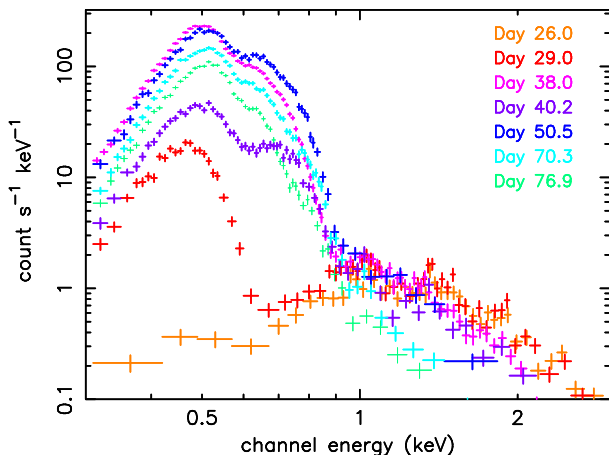


FIG. 3.— The evolution of the *Swift* X-ray spectrum of RS Oph through the outburst. Spectra from various spectral and intensity states are shown with the time after outburst. The spectrum on day 26 shows broad-band emission from the shocked gas and the first detection of a new low-energy component below 0.6 keV, while the day 29 spectrum clearly shows this super-soft source dominating the lower energies. The next two spectra come from the highly variable phase, and show differing flux fractions in the 0.6–1.0 keV band. By day 50, the flux from RS Oph was more stable; the spectra from days 70.3 and 76.9 are taken from the decline phase.

decrease in χ^2 resulting from the inclusion of the second component (addition of a third temperature component does not result in a significantly better fit to any of the spectra); however it is not the purpose of this paper to describe the optically thin shock emission in detail (see Bode et al. 2008; Nelson et al. 2008; Ness et al. 2009).

Analysis of the grating spectra mentioned above (Ness et al. 2007) indicates that neutral oxygen is underabundant in the circumstellar (RG wind) column: $\sim 30\%$ so-

lar around day 40 and 0% by day 54. These values were therefore incorporated into the fits, switching from 30% OI before day 54 to 0% at later times as a simple approximation of the temporal change.

Spectra were extracted for individual orbits of data, between days 26 and 100, to cover the vast majority of the SSS phase. A script was written to fit the spectra automatically within XSPEC. A procedure was defined such that the spectral fits were ‘shaken’ out of local minima wherever possible and the parameters further refined. Despite this, the fits were often statistically poor, with $\chi^2_\nu > 2$, because of the high statistical quality of the data and likely indicating the need for more sophistication in the physical model.

Figure 4 plots the results of the spectral fitting process. The second panel shows how the temperature of the atmosphere model varies over time, starting from the point when the very soft emission was first detected. The third and fourth panels show the radius of the emitting region and the bolometric luminosity, respectively, both estimated from the model atmosphere. The uncertainties on the radius and luminosity are large, typically of order 10–20% (90% confidence) for the radius, and $\sim 40\%$ for the luminosity. The trend changes of the parameters are much larger than the errors on the individual values.

Although the underlying continuum was fairly well approximated by the Rauch atmosphere model, not all of the apparent emission features were accounted for. The Rauch models span abundances with respect to the Sun of carbon = 0.03–0.42 and nitrogen = 64–1.4, reflecting the expectation of CNO processing of accreted material. We used models 003, 004, 007 and 011¹⁷, but our fits did

¹⁷ http://astro.uni-tuebingen.de/~rauch/TMAF/flux_HHeCNOeMgSiS_gen.html. In the framework of

not indicate a preference between them. Figure 4 shows the results from fits to model 003 which has a C/N ratio of 4.8×10^{-4} (i.e., model B of Rauch et al. 2010). The main difference between the fits to the various abundance models was the temperature of the atmosphere after the rapid variability phase (model 011 gave a temperature $\sim 6\%$ lower than that from model 003, and a more gradual cooling after day 60); the best-fit bolometric luminosities were consistent with each other. Nelson et al. (2008) gave a preliminary temperature estimate of $\sim 8.2 \times 10^5$ K (~ 71 eV) for the grating data obtained on day 54, compared to our value of ~ 88 eV. Their value was based on a statistically poor eyeball fit, and this, together with differences in assumed abundances and intrinsic changes in RS Oph, may account for the difference.

The 0.3–10 keV observed (unabsorbed) flux on day 50, around the time of the peak count-rate, was $\sim 5 \times 10^{-9}$ (7×10^{-8}) $\text{erg cm}^{-2} \text{s}^{-1}$, using the Rauch 003 model. This corresponds to a observed band-limited luminosity of $\sim 1.5 \times 10^{36}$ erg s^{-1} (the majority of the total luminosity occurs in the unobservable band below 0.3 keV). The observed flux is completely dominated by the SSS emission: the optically thin components only provide approximately 1% of the flux measured.

Following the interval of high-amplitude variability (see Section 3.1 for a discussion of these data), the temperature of the SSS increases slightly (also shown by the variation of the hardness ratio in Figure 2). This continues until around day 58–60 after outburst, at which point the temperature of the model atmosphere starts to decrease slowly, following the count rate; the cooling becomes more rapid after \sim day 80. The increase in temperature during the early supersoft phase is predicted theoretically (Starrfield et al. 1991; Balman et al. 1998) and should continue until nuclear burning ceases.

Starrfield et al. (1991) gives the radius of a $1.4 M_{\odot}$ WD as 1.9×10^8 cm, which is approximately the minimum effective radius for the SSS measured here, indicating the material has probably all fallen back to an undisturbed WD radius by day 100.

In the past, blackbodies have frequently been used as an approximation to the emission spectrum when fitting supersoft sources. However, such fits can lead to an underestimate of the temperature and an overestimate of the luminosity (e.g., Krautter et al. 1996). Fitting our RS Oph data with blackbodies gave peak temperatures during the ‘plateau’ (between days ~ 40 and 60) of about 65 eV, with a corresponding effective radius of $\sim 7 \times 10^8$ cm and a bolometric luminosity of around $3 \times 10^4 L_{\odot}$, compared to ~ 90 eV, 4×10^8 cm and $3 \times 10^4 L_{\odot}$ derived from the model atmosphere fits. Surprisingly, the plateau blackbody and model atmosphere luminosities are the same; however during the high-amplitude variability phase the blackbody luminosity peaked at $20\text{--}30 \times 10^4 L_{\odot}$, much higher than the model atmosphere peak. The model atmosphere trends

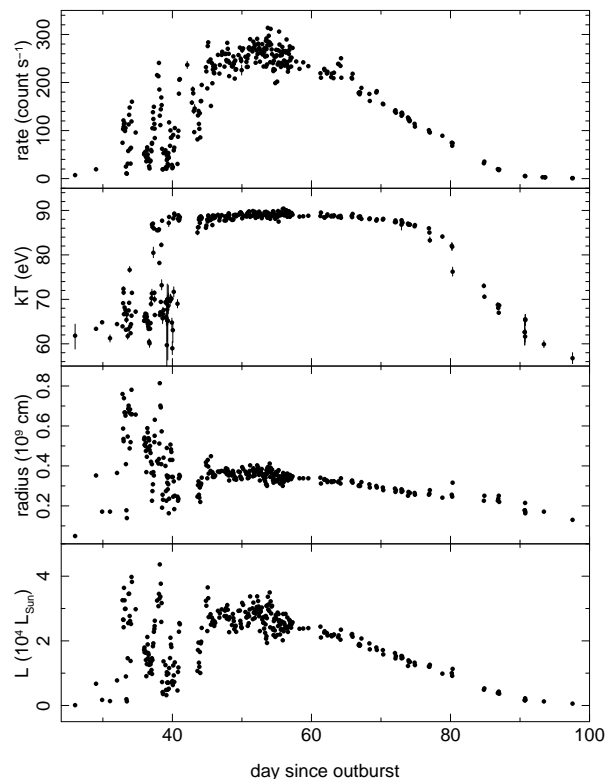


FIG. 4.— Chronological sequence of XSPEC fits of the Rauch atmosphere model grid 003 to the *Swift*-XRT SSS spectra of RS Oph: temperature (second panel), effective radius (third panel) and bolometric luminosity (fourth panel). 30% oxygen was used until the start of day 54, 0% afterwards. The light-curve (top panel) has been binned to have a single point per snapshot. No error bars have been plotted for the radius or luminosity; see text for discussion.

of an initial slight increase in temperature from around day 44 to 55, then a cooling after day 60 or so, together with a short approximately constant luminosity phase followed by fading, were also seen from the blackbody results. Preliminary blackbody fits to the RS Oph data were discussed by Page et al. (2008).

We can compare the luminosities we derive during the SSS phase with other results. Snijders (1987) derived an observed initial luminosity peak for the 1985 outburst about four times the Eddington luminosity (L_{Edd} , the critical luminosity above which radiation pressure exceeds local gravity; this is $4.8 \times 10^4 L_{\odot}$ for a $1.4 M_{\odot}$ WD). There was then a ‘plateau’ at $\sim L_{\text{Edd}}$ for days 8–35 and it took ~ 57 days for the bolometric luminosity to drop by around a factor of two. Iben and Tutukov (1996) give the theoretical relationship of the bolometric luminosity to WD mass during the constant bolometric luminosity (plateau) phase as $L_P \sim 4.6 \times 10^4 (M_{\text{WD}} - 0.26) L_{\odot}$. For $M_{\text{WD}} = 1.4 M_{\odot}$, this gives $L_P \sim 5.2 \times 10^4 L_{\odot}$. The luminosities we find from our spectral fits ($\gtrsim 2\text{--}3 \times 10^4 L_{\odot}$ during the almost-constant count-rate phase, i.e. $\sim L_{\text{Edd}}$) are in gratifying agreement, and are consistent with a high WD mass.

The appearance of the SSS around one month after outburst is predicted by assuming both a constant bolometric luminosity and that the peak of the emission evolves to shorter wavelengths as the effective photospheric radius decreases (caused by the decreasing mass-

the Virtual Observatory (VO; <http://www.ivoa.net>), these spectral energy distributions (SEDs, $\lambda - F_{\lambda}$) are available in VO compliant form via the VO service *TheoSSA* (<http://vo.ari.uni-heidelberg.de/ssatr-0.01/TrSpectra.jsp?>) provided by the *German Astrophysical Virtual Observatory* (GAVO; <http://www.g-vo.org>).

loss rate from the WD; MacDonald, Fujimoto and Truran, 1985). Bath and Harkness (1989) give an expression relating the change in V magnitude from peak, ΔV , to T_{eff} as

$$T_{\text{eff}} = T_0 \times 10^{\Delta V/2.5} K \quad (1)$$

where $T_0 = 8000$ K is the more recent accepted value (Evans et al. 2005, and references therein). By $t = 30$ days, $\Delta V \approx 4.6$ mag¹⁸ and thus $T_{\text{eff}} \approx 5.5 \times 10^5$ K (~ 45 – 50 eV) would be expected at this time. Although this is an approximation (it does not take into account the contribution of nebular emission in the V band, and it assumes that the photosphere emits as a blackbody), the derived value of T_{eff} is in line with our observations, helping to confirm our association of the onset of the SSS phase in RS Oph with the appearance of the nuclear burning source in the XRT band.

3.1. High-amplitude flux variability phase

From shortly after the initial detection of the soft component until about 46 days after the outburst, the X-ray count rate varied dramatically, covering two orders of magnitude. Previous CNe have also shown variability during the super-soft phase. For example, Drake et al. (2003) observed a large, short-lived ‘flare’ during the SSS phase of V1494 Aql. Similarly, Orío et al. (2002) observed a sudden transient flux decrease in V382 Vel with a slight softening of the spectrum, and Ness et al. (2003) found rapid variations and a ‘puzzling episodic turn-off’ accompanied by spectral softening in V4743 Sgr. This behaviour has not yet been explained in the literature. The oscillations cannot readily be ascribed to changes in absorption in neutral intervening gas because of their spectral signature; neither is this behaviour reproduced by existing nova simulations, which do not show variations on these timescales (Starrfield 2008).

While it remains unclear if the variability seen in RS Oph has the same origin as the other cases cited here, it seems likely that our dense observations of RS Oph have discovered a new phenomenon. Since this initial discovery (Osborne et al. 2006b), V458 Vul (Ness et al. 2009), Nova LMC 2009a (Bode et al. 2009; Bode et al. in prep), V2491 Cyg (Ness et al. 2008; Ness et al. 2010) and KT Eri (Beardmore et al. 2010) have all revealed large amplitude variability in their soft X-ray light-curves, remarkably similar to the RS Oph results. One possibility is that clumpiness in the expanding ejected WD envelope could cause variable, and possibly ionized, absorption of the soft X-ray flux between the early total X-ray extinction and the late optically thin phases, broadly consistent with what we have seen in RS Oph. This is investigated in more detail in this section.

Figure 5 shows a short section of the *Swift*-XRT light-curve and hardness ratio. During this time, the emission is typically softer when the source is brighter (see top plot). However, the lower panel highlights snapshots during which the emission hardens as the count rate increases.

The most frequently observed trend of being harder at times of low flux is consistent with variable visibility of the hot white dwarf, at low flux the relatively constant hotter optically thin emission contributes a larger

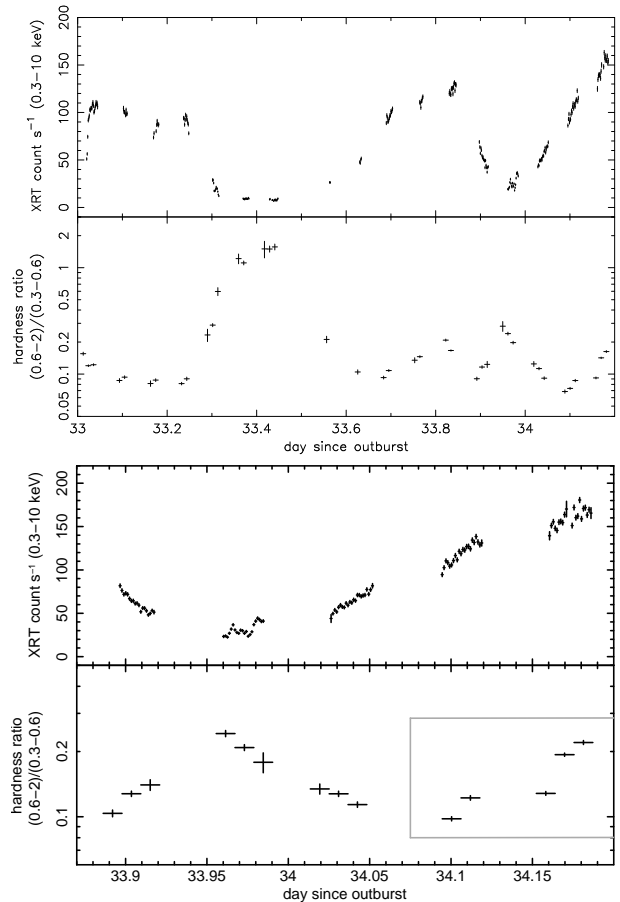


FIG. 5.— The top plot shows the X-ray light-curve and hardness ratio between days 33 and 34.2 after outburst. It can be seen that the general trend is for the X-rays to be softer when the emission is brighter. However, the lower plot zooms in on days 33.9–34.2, demonstrating that some of the snapshots (in the grey box) become harder as the count rate increases.

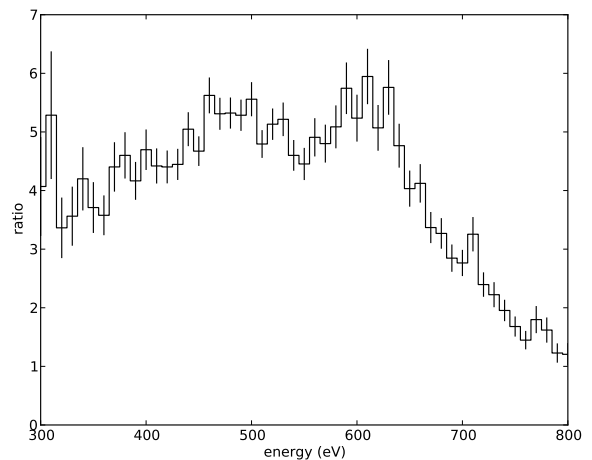


FIG. 6.— The ratio of observed counts per channel spectra from a ‘peak’ and a ‘trough’ of the high amplitude variability phase. The spectral shape of this ratio rules out simple variations in cold absorption or photospheric radius as the cause of the observed flux variations. The spectral resolution is 63 eV FWHM at 500 eV.

¹⁸ <http://www.aavso.org/>

fraction of the observed counts. Photospheric radius variation or variable neutral absorption can in principle account for this behaviour. However a varying photospheric temperature may also be implicated: at low temperatures there is little soft X-ray flux in the XRT band, while the soft count rate increases sharply with higher temperatures so lowering the hardness; at the highest temperatures photospheric flux can appear in the harder spectral band causing the hardness to rise. In addition to these possibilities, variable ionization of the absorbing medium may play a role, allowing softer flux to escape when it is more highly ionized.

Figure 6 shows the ratio of a ‘bright’ and a ‘faint’ spectrum during this interval of variability and demonstrates that we are probably seeing a combination of effects. It appears to rule out both a variable neutral absorption and a radius change as neither would show a declining ratio to lower energies. Variations in the ionization state of realistic ionized wind absorption also do not show a declining spectral ratio to lower energies. An increased photospheric temperature when brighter does produce a spectral ratio qualitatively similar to that of Fig. 6, especially in combination with decreased radius, but we have been unable to find a good quantitative match to this ratio using our fitted model atmospheres and shock models.

If the absorption is changing in some complex fashion during this phase of the evolution, then constraining the column to decay as $N_{\text{H,wind}} = 7.5 \times 10^{21} \text{ t}^{-0.5} \text{ cm}^{-2}$ (Section 3) may be an inappropriate approximation. Repeating the fits with a varying $N_{\text{H,wind}}$ presented the same overall trends, however.

High resolution X-ray grating spectra can be valuable in diagnosing the large flux modulation (e.g. see sect. 3.5 of Ness et al. 20007), although a persuasive physical explanation for this remains to be found.

4. RAPID QUASI-PERIODIC VARIABILITY

A strong short-period modulation of the soft X-ray flux was seen during much of the SSS phase (Osborne et al. 2006b). This modulation was first detected on day 32.9 and continued until last detected on day 58.8, coincident with the onset of the flux decline (see Fig. 7). Soft X-ray light curves in the band 0.3–1 keV were created with 1 s binning, with a duration of 1024 seconds and at least 75% exposure for all WT mode observations (i.e. up to day 90) in order to characterise this modulation via Fourier transforms. We verified by simulations that the oscillations in the X-ray flux were not strictly periodic, ruling out rigid rotation of the WD as the origin. Although the excess Fourier power in the entire dataset was centred on 35.3 s, detected periods formed a distribution with FWHM points at 34.5 and 38.5 s before day 49, but only between the adjacent frequency bins corresponding to periods of 34.7 and 35.9 s after that date (see top panel of Fig. 8). Periods and coherence were measured by fits to the power spectra; we found $P = 35.82 \pm 0.06 \text{ s}$ for all the data before day 49 and $P = 34.88 \pm 0.02 \text{ s}$ after; the 1σ ranges quoted here reflect the distribution of power rather than measurement error; the coherence of the signal is a factor of three poorer in the earlier data. The modulation amplitude varied up to $\sim 10\%$; neither the modulation amplitude nor the period were correlated with intensity (Beardmore et al. 2008). The lower panel

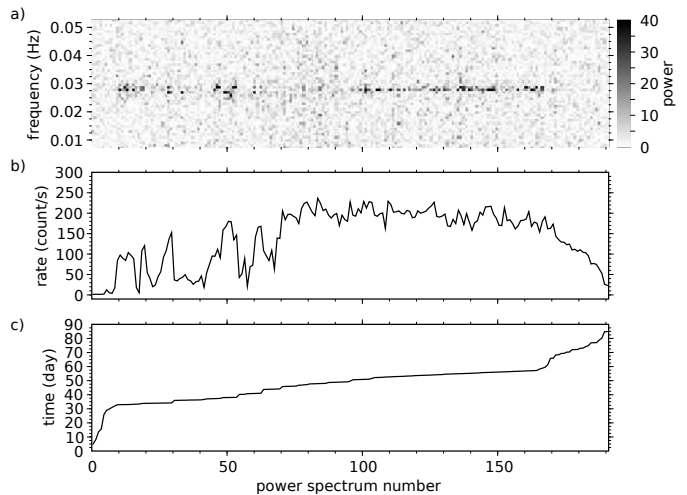


Fig. 7.— Oscillatory modulation of the soft X-ray flux of RS Oph. a) Fourier power spectra for successive observations; each power spectrum is constructed from a 1024 s light curve of 1 second binning in the 0.3–1.0 keV band and the unbinned Fourier power is shown on a linear grey scale. b) The source intensity in each power spectrum. c) The relation between time and the power spectrum index number (used as the x-axis of each plot); time does not increase uniformly as we have suppressed times when there were no observations. Sporadic power can be seen between frequencies of 0.026 and 0.029 Hz, corresponding to periods of 34.5 to 38.5 s. While the modulation is generally present when RS Oph is bright, counter-examples can be seen around bins 33 (day 36.0) and 45 (day 37.2), and the modulation is no longer present after bin 167 (day 58.8).

of Fig. 8 illustrates the modulation during $\sim 830 \text{ s}$ on day 37.2, when it was particularly strong. The modulation was primarily sinusoidal, occasionally showing a first harmonic; there is no detectable spectral variation. Comparison of spectral fits using the 003 model atmosphere to spectra accumulated over 0.2 cycle phase intervals at the phases of maximum and minimum flux did not show temperature changes above 2%. More details are provided by Beardmore et al (2008), who also illustrate the 35 s flux variation in the light-curve and the simultaneous presence of multiple periods¹⁹. The 35 s modulation was also seen in contemporaneous *XMM-Newton* data (Ness et al. 2007).

This $\sim 35 \text{ s}$ periodicity is by far the shortest period seen in the SSS phase of a nova to-date, although periodic oscillations have been observed in other novae during this phase ($P = 22 \text{ min}$ in V4743 Sgr, Ness et al. 2003; $P = 42 \text{ min}$ amongst others in V1494 Aql, Drake et al. 2003). A period of 38 min has also been seen in the X-ray flux of the persistent super-soft source CAL 83 (Schmidtke & Cowley 2006). These longer period oscillations have been ascribed to g+-mode (buoyancy) pulsations driven by an ionisation-opacity instability such as occurs in pulsating planetary nebulae nuclei (PNN) or GW Vir stars (Drake et al. 2003). It has however been noted (Drake et al. 2003) that the so-called ϵ -mechanism could be responsible and this should produce much shorter periods (these are oscillations in which increased nuclear energy generation is followed by expansion leading to a reduced

¹⁹ The current paper updates the statements regarding spectral variation in this reference.

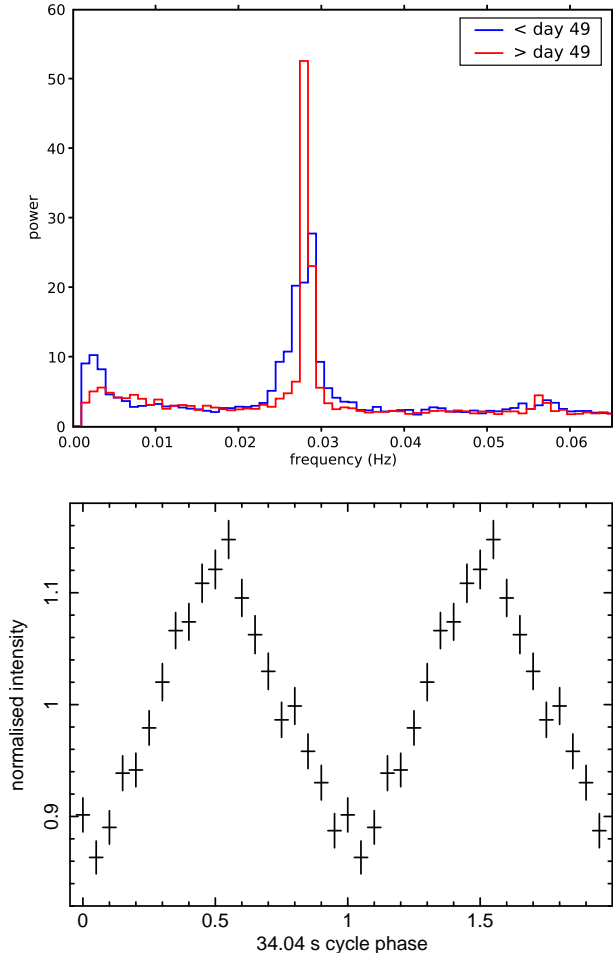


FIG. 8.— The ~ 35 s quasi-period of RS Oph. Top plot: Fourier power spectra of the aggregated light curves used in Fig. 7, showing the increased coherence of the 35 s modulation after day 49. A weak harmonic can be seen at 0.056 Hz; aperiodic red noise is visible at the lowest frequencies. Bottom plot: Normalised soft X-ray light curve from day 37.2, when the modulation was particularly strong, folded at the period then present.

generation rate which is followed by contraction which leads to an increased rate); such oscillations could be manifest at the SSS photosphere as cyclic changes in radius and or temperature. Kawaler (1988) finds periods of 70–200 s from this mechanism for a $0.62 M_{\odot}$ PNN and one expects the period, P , to decrease with the mass of the WD (e.g. if $P \propto \rho_m^{-0.5}$, where ρ_m is the mean density of the WD from Starrfield et al. [1991], then $M_{WD} \sim 0.9\text{--}1.25 M_{\odot}$). Such oscillations might therefore be the source of the modulation we see in RS Oph in the SSS phase: they would only last as long as the nuclear burning source was still active on the WD surface, as is observed. This reinforces the proposition that nuclear burning is the origin of the SSS emission prior to the decline, at which point the oscillations in RS Oph cease, if the decline is due to the cessation of widespread nuclear fusion. Since the models of Kawaler relate to $L < 1600 L_{\odot}$ and have long instability growth times, further work is required to establish whether the ϵ -mechanism is indeed responsible for the short period modulation we have seen.

If this turns out to be the case, then we can expect strong constraints on the mass and structure of the WD.

We consider that Dwarf Nova Oscillations (DNO), which typically have periods ~ 30 s, are unlikely to be related to the modulations we have detected. Ascribed to the accretion disk-WD boundary layer in dwarf novae and some nova-like binaries, models of DNO depend on a form of magnetically controlled accretion loosely tied to the body of the WD (Warner 2004). The high luminosity of RS Oph during the SSS phase rules out an accretion-related origin of the 35-s period. Also ruled out is an intermediate polar mechanism, since the same luminosity argument applies, and the period changes seen are not consistent with realistic torques on the WD.

Swift observations of KT Eri (Nova Eri 2009) also revealed a ~ 35 s modulation (Beardmore et al. 2010), with fractional amplitudes of up to 7%; as in RS Oph the periodicity was not continuously present. The existence of a very similar modulation in two different novae adds weight to the tentative conclusion that this period does not have a rotation-based origin, and the surprising similarity of the (very short) periods might suggest that both objects contain WDs near the Chandrasekhar limit.

5. MASS AND LUMINOSITY IN THE RS OPH SYSTEM

In this section, we obtain estimates of the fundamental parameters for RS Oph. The timing of the start of the final decline (i.e., day 58) is an important parameter. The turn-off time for nuclear burning, t_{rem} , is a steep function of WD mass; MacDonald (1996) finds, for example, $t_{\text{rem}} \propto M_{WD}^{-6.3}$. The fact that the deduced nuclear burning timescale in RS Oph is much shorter than that observed in other novae (e.g. V1974 Cyg, where $t_{\text{rem}} \gtrsim 511$ days and $M_{WD} \sim 1.2 M_{\odot}$ [Krautter et al. 1996; Balman et al. 1998]) is thus consistent with the existence of a much higher mass WD in RS Oph. Furthermore, from Starrfield et al. (1991), the observed turn-off timescale in RS Oph implies $M_{WD} \sim 1.35 M_{\odot}$ (see also Hachisu et al. 2007).

The critical mass of the accreted envelope required to trigger a thermonuclear runaway is given by

$$M_{\text{acc}} \approx \frac{4\pi R_{WD}^4 P_{\text{crit}}}{GM_{WD}} \quad (2)$$

(Truran & Livio 1986), where $P_{\text{crit}} \sim 10^{20}$ dyne cm^{-2} for $M_{WD} = 1.4 M_{\odot}$. Thus with $R_{WD} = 1.9 \times 10^8$ cm (Starrfield et al. 1991), $M_{\text{acc}} \approx 4.4 \times 10^{-6} M_{\odot}$. This estimate of the accreted mass necessary for outburst is in line with the results of numerical simulations of the recurrent nova outburst using solar abundance material (Starrfield et al. 1988) and the estimate of Hachisu et al. (2007). We may compare this to the mass burnt, M_b , from

$$M_b = \frac{E_{SE} + E_p + E_{LO} + \Delta E_{KE} - E_{CE}}{X\epsilon_H} \quad (3)$$

where E_{SE} is the luminous energy in the initial super-Eddington phase with luminosity L_{SE} lasting t_{SE} days; $E_p = L_p(t_{\text{rem}} - t_{SE})$ is the luminous energy in the constant luminosity ‘plateau’ phase; $E_{LO} = (GM_{WD}\Delta M)/R_{WD}$ is the energy required to lift off the ejected mass, ΔM ; ΔE_{KE} is any additional kinetic

energy given to the ejecta; E_{CE} is the energy imparted to the expanding envelope by the secondary star in the so-called common envelope stage where the ejecta envelop the secondary; X is the mass fraction of hydrogen and $\epsilon_H = 6.4 \times 10^{18} \text{ erg g}^{-1}$.

From the observational and theoretical considerations of the nuclear burning phase given above, we take $L_p = 2.5 \times 10^4 L_\odot$ and $t_{\text{rem}} = 58$ days. With $L_{SE} \sim 2 \times 10^5 L_\odot$ and $t_{SE} \sim 7$ days, derived from the 1985 outburst, $E_{SE} = 4.8 \times 10^{44} \text{ erg}$ and $E_p = 2.5 \times 10^{44} \text{ erg}$. Using the WD parameters above, $E_{LO} = (2-20) \times 10^{44} \text{ erg}$ for $\Delta M = 10^{-7}-10^{-6} M_\odot$ (Hjellming et al. 1986; O'Brien et al. 1992; Sokoloski et al. 2006). From the results of the shocked wind model fits to the 1985 outburst data (O'Brien et al. 1992), ΔE_{KE} appears negligible in comparison (although more recent modelling by Vaytet et al (2010) yields energies more comparable to those from the plateau, see also Orlando et al. 2009). E_{CE} is insignificant for this wide binary. We therefore conclude that $M_b = (1-3) \times 10^{-7} M_\odot$ (for $X = 0.7$, since the matter from the RG will be relatively H-rich). Thus the mass burnt is a few percent of the mass of the accreted envelope.

We now turn to the monotonic decline following the plateau phase. Krautter et al. (1996) suggested that the decline they saw in V1974 Cyg was consistent with energy radiated from gravitational contraction of the extended WD atmosphere, comprising material not ejected at the time of outburst, once the nuclear burning source was extinguished. A gradual softening of the source was also noted, as seen in RS Oph at this stage (see Fig. 2), consistent with cooling of the emitting region. From consideration of the Kelvin-Helmholtz timescale, τ_K , associated with the contraction of this envelope, mass M_A , it can be shown that

$$M_A = \left(\frac{4R_{WD}}{3GM_{WD}} \right) L_p \tau_K \quad (4)$$

Thus with $\tau_K \sim 1$ month, and L_p , M_{WD} and R_{WD} as above, $M_A \sim 1 \times 10^{-7} M_\odot$. Both M_b and M_A are less than M_{acc} as expected, and our value of M_A is much less than $\sim 10^{-5} M_\odot$ found for the classical nova V1974 Cyg (Krautter et al. 1996) – again implying that the WD in RS Oph is much more massive than the $\sim 1.2 M_\odot$ WD in V1974 Cyg.

With the accreted mass between outbursts $M_{\text{acc}} \approx 4.4 \times 10^{-6} M_\odot$ and the ejected mass at outburst $\Delta M = 10^{-7}-10^{-6} M_\odot$, we confirm the conclusion of Hachisu et al. (2007) that matter is gradually accumulating on the extremely high mass WD in RS Oph. Thus, it seems that the WD is growing in mass to the Chandrasekhar limit, leading to its ultimate demise as a (possible) Type Ia supernova (as also predicted for U Sco by Starrfield et al. 1988).

Marietta et al. (2000) have shown that entrainment of secondary star hydrogen during the supernova explosion may reveal itself as low velocity lines becoming visible in the late stages of an explosion which, however, have never been seen in a Type Ia explosion. Hachisu et al. (2007) also conclude that RS Oph will explode in this way, based on the same *Swift* observations as presented here. Against this, the recent work of Hayden et

al. (2010) shows that red giants are disfavoured as the companions of SN Ia progenitors. Another major uncertainty is the nature of the WD; if the WD is originally of the ONe type rather than CO, and matter is added to take it beyond the Chandrasekhar limit, an implosion will occur rather than a supernova explosion. Thus the WD type is crucial to determining the ultimate fate of the RS Oph system. The key here may come from abundance analyses of spectroscopy taken both before and during the outburst. This is discussed in more detail in terms of the results of high resolution X-ray spectroscopy from *Chandra* and *XMM-Newton* by Ness et al. (2009).

Finally, from M_{acc} and the inter-outburst (1985 to 2006) period, we derive a mean accretion rate $\dot{M}_{\text{acc}} = 2 \times 10^{-7} M_\odot \text{ yr}^{-1}$. We note that this is very similar to the net mass-loss rate in the red giant wind escaping the system derived in Hjellming et al. (1986: $\dot{M}_{\text{RG}} = 8 \times 10^{-8}-2.4 \times 10^{-7} M_\odot \text{ yr}^{-1}$ for $v_{\text{wind}} = 10-20 \text{ km s}^{-1}$), but much lower than the $1.8 \times 10^{-6} M_\odot \text{ yr}^{-1}$ derived by Bohigas et al. (1989). Using

$$L_{\text{acc}} = (1 - \alpha) \frac{GM_{WD} \dot{M}_{\text{acc}}}{2R_{WD}} \quad (5)$$

where $\alpha = 0.5$ (Starrfield et al. 1988; see also Popham & Narayan 1985), we find a mean observable inter-outburst accretion luminosity, $L_{\text{acc}} = 3.1 \times 10^{36} \text{ erg s}^{-1}$. Spectral fits to our *Swift* data at the very latest epochs give $L_X \sim \text{few} \times 10^{31} \text{ erg s}^{-1}$, suggesting that accretion is not yet fully re-established. This *Swift* measurement is of the same order as the X-ray luminosity of $(3-20) \times 10^{31} \text{ erg s}^{-1}$ derived from *ROSAT* observations some years after the 1985 outburst (Orion 1993), with the flux from our late-time spectral fit being of the same order of magnitude as the upper bound of the *ROSAT* estimate. Such a low value has yet to be explained in our understanding of the evolution of RS Oph, this subject is examined by Mukai (2008) who speculates that the mass-accumulating white dwarf would be highly spun up, thus suppressing the boundary layer X-ray luminosity. In any case, to determine L_{acc} accurately, observations at lower energies (UV and optical) are also needed. Indeed, we note that Snijders (1987) found a much higher accretion luminosity, around that required, from analysis of IUE observations during quiescence of RS Oph before the 1985 outburst.

6. SUMMARY

Our *Swift* X-ray observations of the 2006 outburst of the recurrent nova RS Oph have shown it to be the brightest SSS yet observed, and have followed the progress of the nuclear burning source on the surface of the white dwarf in unprecedented detail. First seen on day 26, the super-soft phase started with a phase of extreme variability; the flux stabilised around day 46 at around L_{Edd} and began a decline around day 58. This high-amplitude variability may be a product of both varying temperature and ‘blobby’, possibly ionized, absorption. During days 33–59, a $\sim 35 \text{ s}$ modulation was seen, which became increasingly coherent through this interval.

From these observations we have confirmed the basic model of the outburst and, more importantly, concluded

that this may be a progenitor system for a future supernova event, the main uncertainty being the nature of the white dwarf. However, our discoveries pose further observational and theoretical challenges. These include understanding the nature of the short period oscillations and the early extreme variability uncovered by our observations, as well as confirming observationally the mass accretion rate we predict to be required to give rise to the next explosion.

7. ACKNOWLEDGMENTS

We thank the *Swift* Science Team and the *Swift* Mission Operations Team for their excellent support of this observing campaign. JO, KP, MG, AB, MFB acknowledge the support of STFC. SS acknowledges partial support to ASU from NSF and NASA. TR is supported by the German Aerospace Center (DLR) under grant 05OR0806. The authors are grateful to John Nousek for his helpful comments on an initial draft of this paper and to Simon Vaughan for providing the TCL ‘shakefit’ procedure.

REFERENCES

- Balman, S., Krautter, J. & Ögelman, H. 1998, *ApJ*, 499, 395
 Banerjee, D., Das, R.K. & Ashok, N.M. 2009, *MNRAS*, 399, 357
 Barthelmy, S.D., et al. 2005, *Space Sci. Rev.* 120, 143
 Bath, G.T. & Harkness, R.P. 1989, in *Classical Novae*, ed. M.F. Bode & A. Evans (Wiley: Chichester), 61 [First Edition]
 Beardmore A.P., et al. 2008, in *RS Ophiuchi (2006) and the Recurrent Nova Phenomenon*, eds A. Evans, M. Bode, T. O’Brien, M.Darnley. ASP Conf Ser, 401, 296
 Beardmore A.P., et al. 2010, *The Astronomer’s Telegram*, 2423
 Bode, M.F. 1987, in *RS Ophiuchi (1985) and the Recurrent Nova Phenomenon*, ed. M.F. Bode (VNU Science Press: Utrecht), 241
 Bode, M.F., et al. 2006, *ApJ*, 652, 629
 Bode, M.F., et al. 2007, *ApJ*, 665, L63
 Bode, M.F., et al. 2008, in *RS Ophiuchi (2006) and the Recurrent Nova Phenomenon*, eds A. Evans, M.F. Bode, T.J.O’Brien, M.J.Darnley. ASP Conf Ser 401, 269
 Bode, M.F., et al. 2009, *The Astronomer’s Telegram*, 2025
 Bohigas, J., Echevarria, J., Diego, F., Sarmiento, J.A. 1989, *MNRAS*, 238, 1395
 Brandi, E., Quiroga, C., Mikołajewska, J., Ferrer, O.E., García, L.G. 2009, 497, 815
 Burrows, D.N., et al. 2005, *Space Sci. Rev.* 120, 165
 Chesneau O. et al. 2007, *A&A*, 464, 119
 Das, R., Bannerjee, D.P.K. & Ashok, N.M. 2006, *ApJ*, 653, L141
 Drake, J.J., et al. 2003, *ApJ*, 584, 448
 Drake, J.J., et al. 2009, *ApJ*, 691, 418
 Evans, A., Tyne, V.H., Smith, O., Geballe, T.R., Rawlings, J.M.C. & Eyres, S.P.S. 2005, *MNRAS*, 360, 1483
 Evans, A. et al. 2007a, *MNRAS*, 374, L1
 Evans, A. et al. 2007b, *ApJ*, 663, L29
 Eyres, S.P.S. et al. 2009, *MNRAS*, 395, 1533
 Gehrels, N., et al. 2004, *ApJ*, 611, 1005
 Hachisu, I., Kato, M., & Luna, G.J.M. 2007, *ApJ*, 659, L153
 Hachisu, I. et al. 2006, *ApJ*, 651, L141
 Hayden, B.T., et al. 2010, *ApJ*, 722, 1691
 Hjellming, R.M., et al. 1986, *ApJ*, 305, L71
 Hounsell, R. et al. 2010, *ApJ* in press (arXiv:10091737)
 Iben, I. & Tutukov, A.V. 1996, *ApJS*, 105, 145
 Kantharia, N.G., Anupama, G.C., Prabhu, T.P., Ramya, S., Bode, M.F., Eyres, S.P.S., O’Brien, T.J. 2007, *ApJ*, 667, L171
 Kawaler, S.D. 1998, *ApJ*, 334, 220
 Krautter, J., Ogelman, H., Starrfield, S., Wichmann, R. & Pfeffermann, E. 1996, *ApJ*, 456, 788
 Lane, B.F. et al. 2007, *ApJ*, 658, 520
 Luna, G.J.M., Montez, R., Sokoloski, J.L., Mukai, K., Kastner, J.H. 2009, *ApJ*, 707, 1168
 MacDonald, J., Fujimoto, M.Y., & Truran, J.W. 1985, *ApJ*, 294, 263.
 MacDonald, J. 1996, in *Cataclysmic variables and related objects*, IAU Colloquium 158, ed. A. Evans & J.H. Wood (Kluwer Academic Publishers: Dordrecht), 281
 Marrietta, E., Burrows, A. & Fryxell, B. 2000, *ApJS*, 128, 615.
 Mason, K.O., Cordova, F.A., Bode, M.F., Barr, P. 1987, in *RS Ophiuchi (1985) and the recurrent nova phenomenon*, VNU Science Press, Utrecht, ed. M.F. Bode
 Monnier, J.D. et al. 2006, *ApJ*, 647, L127
 Mukai, K. in *RS Ophiuchi (2006) and the Recurrent Nova Phenomenon*, eds A. Evans, M.F. Bode, T.J.O’Brien, M.J.Darnley. ASP Conf Ser 401, 84
 Munari, U. et al. 2007, *BaltA*, 16, 46
 Narumi, H. et al. 2006, *IAUC* 8671
 Nelson, T., Orio, M., Cassinelli, J.P., Still, M., Leibowitz, E., & Mucciarelli, P. 2008, *ApJ*, 673, 1067
 Ness, J.-U. et al., 2010, *MNRAS*, submitted
 Ness, J.-U. et al. 2009, *AJ*, 137, 3414
 Ness, J.-U. et al. 2008, *The Astronomer’s Telegram*, 1561
 Ness, J.-U. et al. 2007, *ApJ*, 665, 1334
 Ness, J.-U., et al. 2003, *ApJ*, 594, L127
 O’Brien, T.J., Bode, M.F., & Kahn, F.D. 1992, *MNRAS*, 255, 683
 O’Brien, T.J. et al. 2006, *Nature*, 442, 279
 Orio, M. 1993, *A&A*, 274, L41
 Orio, M., et al. 2002, *MNRAS*, 333, L11
 Osborne, J.P., et al. 2006a, *The Astronomer’s Telegram*, 764
 Osborne, J.P., et al. 2006b, *The Astronomer’s Telegram*, 770
 Osborne, J.P., et al. 2006c, *The Astronomer’s Telegram*, 801
 Osborne, J.P., et al. 2006d, *The Astronomer’s Telegram*, 838
 Page, K.L., et al. 2010, *MNRAS*, 401, 121
 Page, K.L., et al. 2008, in *RS Ophiuchi (2006) and the Recurrent Nova Phenomenon*, eds A. Evans, M. Bode, T. O’Brien, M.Darnley, ASP Conf Ser, 401, 283
 Popham, R. & Narayan, R. 1995 *ApJ*, 442, 337
 Rauch, T. 2003, *A&A*, 403, 709
 Rauch, T., Orio, M., Gonzales-Riestra, R., Nelson, T., Still, M., Werner, K., Wilms, J. 2010, *ApJ*, 717, 363
 Roming, P.W.A., et al. 2005, *Space Sci. Rev.* 120, 95
 Rushton, M.T. et al. 2010, *MNRAS*, 401, 99
 Schaefer, B.E. 2010, *ApJS*, 187, 275
 Snijders, M.A.J. 1987, in *RS Ophiuchi (1985) and the Recurrent Nova Phenomenon*, ed. M.F. Bode (VNU Science Press: Utrecht), 51
 Sala, G., & Hernanz, M. 2005, *A&A*, 439, 1061
 Schmidtke, P.C., & Cowley, A.P. 2006, *ApJ*, 131, 600
 Sokoloski, J.J., Luna, G.J.M., Mukai, K., & Kenyon, S.J. 2006, *Nature*, 442, 276
 Sokoloski, J.J., Rupen, M.P., & Mioduszewski, A.J. 2008, *ApJ* 685, L137
 Starrfield, S., Sparks, W.M. & Shaviv, G. 1988, *ApJL*, 325, 35
 Starrfield, S. 2008, in *Classical Novae*, 2nd Ed., ed. M. Bode & A. Evans (CUP: Cambridge), 77
 Starrfield, S., Truran, J.W., Sparks, W.M. & Krautter, J. 1991, in *Extreme Ultraviolet Astronomy*, ed. R.F. Malina & S. Bowyer (Pergamon Press: Oxford), 168
 Townsley, D.M., 2008, ASP conf ser, 401, 131, in *RS Ophiuchi (2006) and the Recurrent Nova Phenomenon*, eds A. Evans, M.F. Bode, T.J. O’Brien, M.J. Darnley
 Truran, J. & Livio, M. 1986, *ApJ*, 308, 721
 Vaytet, N.M.H., O’Brien, T.J. & Bode, M.F. 2007, *ApJ*, 665, 654
 Vaytet, N.M.H. et al. 2010, *ApJ* submitted
 Warner, B. 2004, *PASP*, 116, 115
 Worters, H.L., Eyres, S.P.S., Bromage, G.E. & Osborne, J.P. 2007, *MNRAS*, 379, 1557